

ULTRA-HIGH STRENGTH TWIP STEEL WITH HIGH CHROMIUM CONTENT

PAVEL PODANY¹, TOMAS STUDECKY¹, TOMAS GREGOR¹,
RADEK PROCHAZKA¹, ALEKSANDRA KOCIJAN²

¹COMTES FHT a.s., Dobruška, Czech Republic

²IMT – Institute of Metals and Technology, Ljubljana, Slovenia

DOI: 10.17973/MMSJ.2023_06_2023041

e-mail: pavel.podany@comtesfht.cz

A new ultra-high strength steel with a fully austenitic microstructure and twinning-induced plasticity (TWIP) effect has been developed. TWIP effect gives this steel a good combination of high strength of over 1000 MPa and ductility of over 35%. This new steel has a high chromium content, which increases its corrosion resistance. By combining cold rolling and annealing, the steel has achieved a very fine austenitic microstructure with an average grain diameter of 2.85 μm . This steel could be used for structural applications or components that need to withstand high levels of stress, deformation and corrosion environment.

KEYWORDS

TWIP steels, corrosion resistance, microstructure, tensile strength, plasticity

1 INTRODUCTION

TWIP steels are high strength, high ductility austenitic steels with a high degree of strengthening due to the twinning mechanism [Cooman 2018]. The combination of high strength, ductility and very good impact resistance makes TWIP steels a promising material, especially for the automotive industry [Kwon 2010]. In the event of a collision, bodies made from TWIP steels deform while retaining their plasticity - important for the distribution and absorption of impact energy. The energy is absorbed much more efficiently, and the occupants have a better chance of survival [Cornette 2005]. The chromium content in TWIP steels has a positive effect on the yield strength and tensile strength, whereby as the Cr content of the matrix increases, the average grain size decreases and the amount of intragranular precipitated Cr_{23}C_6 phases increases [Yuan 2017]. Several studies can be found in the literature on TWIP steels with improved corrosion resistance, where the chromium content ranges from 2 to 12 wt.% and is often combined with aluminium alloying [Saad 2007, Mujica Roncery 2012, Mujica 2011, Tsay 2010]. At present, there are very few studies on high chromium fully austenitic TWIP steels. No study was found in the literature dealing with TWIP steels with chromium contents above 12% together with tensile strength above 1000 MPa. This paper deals with the brief description of research and development of TWIP steel with tensile strength above 1000 MPa and increased corrosion resistance due to the chromium alloying above 14 wt.%.

2 MATERIALS AND METHODS

An experimental steel melt was cast (see Tab. 1 for chemical composition). The steel was melted in an induction furnace and cast into a 50 kg ingot. The ingot was then heated to a rolling temperature of 1100 °C with a dwell time of 2 hours, from

which it was hot rolled on a rolling mill to a sheet thickness of 10 mm. This was followed by milling to remove scales from the surface. This sheet was cold rolled to a thickness of 4 mm. The semi-rolled product was recrystallization annealed in a vacuum furnace at 925°C for 2 hours. Samples were taken from the final sheet for mechanical properties testing, metallographic evaluation and X-ray diffraction of the phase composition. Samples for X-ray diffraction (XRD) were also taken from the cold-rolled sheet prior to recrystallization annealing. Metallographic specimens were prepared using standard procedures: mechanical grinding on sandpapers, polishing with diamond suspensions and final chemical polishing with Struers OP-5 colloidal silica suspension. Several reagents were used with no success for revealing the microstructure for observation by means of light microscope. Partial success was only reached with V2A reagent (hydrochloric acid, nitric acid and water) with slight attack of grain boundaries and carbides. Therefore, the JEOL IT 500 HR scanning electron microscope was also used to observe the microstructure. The microstructure was captured on the as-polished sample using a sensitive backscattered electron detector at a low observation distance of 5 mm and an acceleration voltage of 5 kV. This setup ensures good microstructure images with visible grains and their twins. Electron Backscattered Diffraction (EBSD) analysis using the HIKARI Super EBSD camera from EDAX™ was used for grain size characterisation. EBSD data analysis was performed using EDAX OIM analysis software. Tensile tests were performed on an electromechanical testing machine. Strain was measured using a strain gauge extensometer. Characteristic dimensions were measured before and after the test.

Heat	C	Mn	Cr	Si	Mo	N	S
T22	0.37	29.4	14.5	0.15	0.51	0.47	0.001

Table 1. Chemical composition of experimental steel

An experimental steel specimen with a metallographically polished surface was used to measure the corrosion properties. The test was carried out at 21°C in model seawater containing 3.5 wt.% NaCl. The Gamry PC4 electrochemical potentiostat was used for the measurements. The samples were stabilised at the open circuit potential (Eoc) for 3600 s. The polarisation resistance (Rp) was measured within ± 0.02 V/Eoc at a scan rate of 0.125 mV/s. The cyclic polarisation curve was measured in the range of $-0.2\text{V}/\text{Eoc}$ to $1.2\text{V}/\text{Eoc}$ at a scan rate of 0.5 mV/s. A pressure cell was used for the measurements. A Pt counter electrode and a silver chloride reference electrode (ACLE) were used for all measurements.

3 RESULT AND DISCUSSION

3.1 Microstructure

X-ray diffraction of the sheet specimens before and after recrystallization annealing Fig. 1 showed that the phase composition in both the annealed and cold deformed states correspond to a fully austenitic microstructure without the presence of transformation-induced martensite (alpha or epsilon). Small peaks to the right and left of peak (111) γ indicate the presence of a carbide Cr_{23}C_6 phase.

The absence of alpha or epsilon martensite in this experimental steel is very important. That is because the presence of hard

martensite phases in these steels increases the susceptibility to delayed fracture due to hydrogen [Cooman 2018].

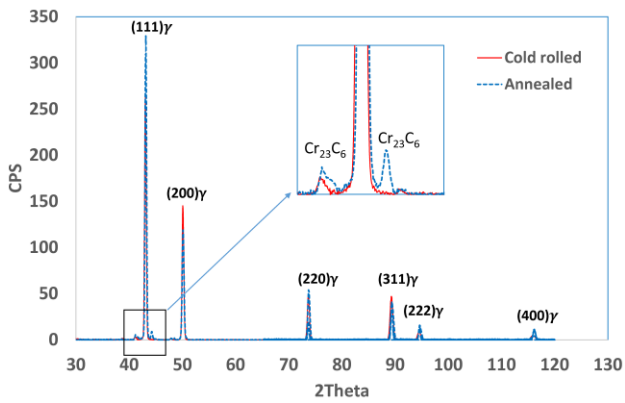


Figure 1. XRD patterns after cold rolling and annealing

The microstructure after etching with V2A reagent is shown in the Fig. 2. There were partially revealed the grain boundaries and the presence of $Cr_{23}C_6$ carbides.

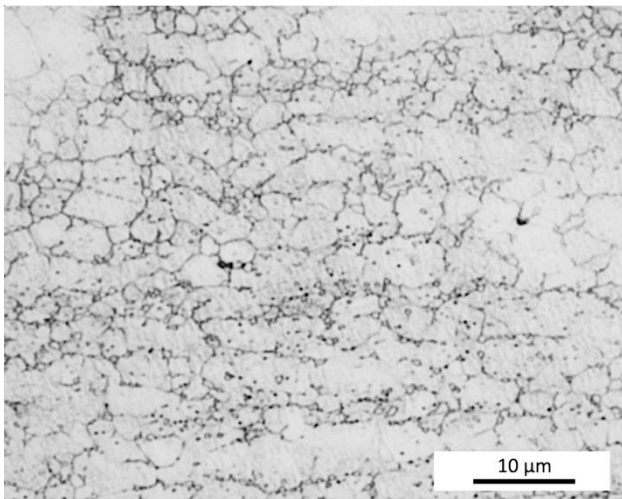


Figure 2. Microstructure of the steel etched with V2A reagent and observed by means of light microscope

The electron backscattered mode microstructure image Fig. 3 clearly shows the presence of fine $Cr_{23}C_6$ carbides in the microstructure.

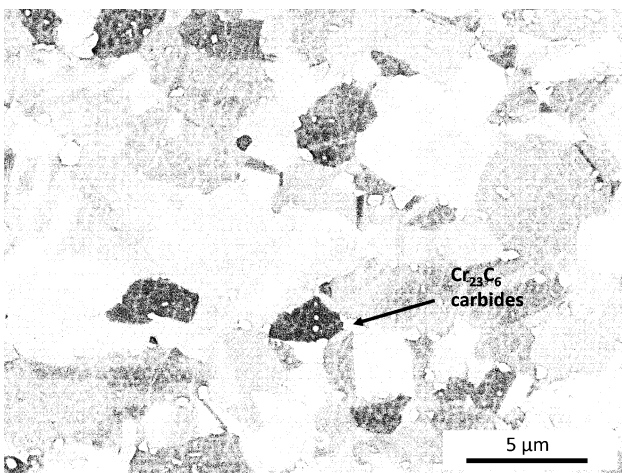


Figure 3. Microstructure of the steel with visible carbides (SEM)

EBSD IPF (inverted pole figures) map of the sample taken from the sheet in the state after recrystallization annealing (Fig. 4)

shows the homogenous microstructure of the austenitic grains with twins.

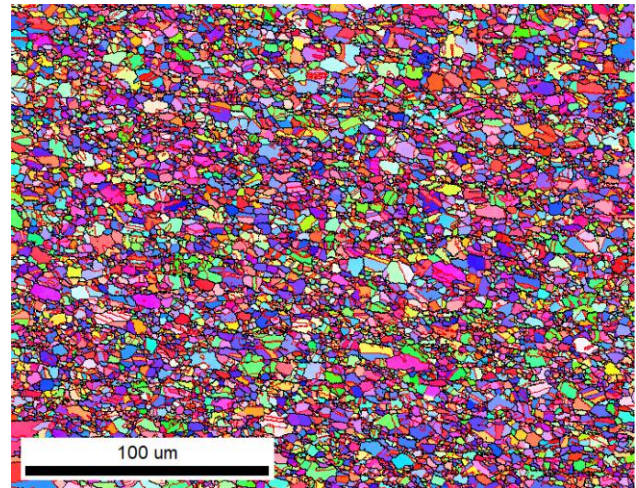


Figure 4. EBSD IPF coloured map of the annealed state

The average grain diameter reaches only 2.85 μm . It is $G = 15.1$ according to ASTM E112 (Standard Test Methods for Determining Average Grain Size). It demonstrates a very fine microstructure obtained by intensive cold forming (with reduction over 50%) and a suitably chosen recrystallization annealing temperature. The distribution of grains is homogeneous throughout the thickness of the sheet and no defects or banding are evident (see Fig. 5).

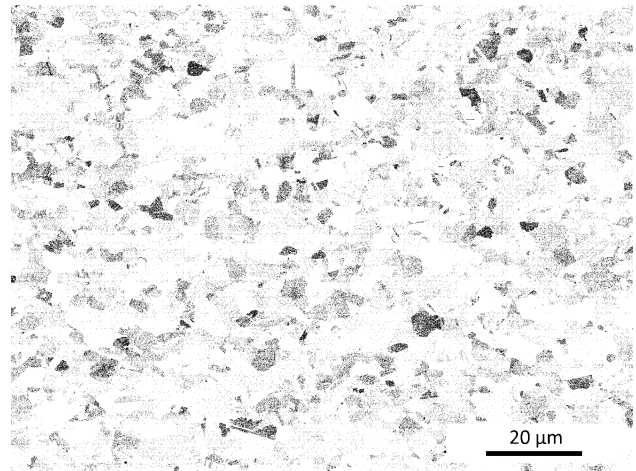


Figure 5. Microstructure of the steel with uniformly distributed fine grains (SEM)

3.2 Mechanical properties

The mechanical properties were tested on three specimens that were taken from the sheet after the recrystallisation annealing process. Yield strength (YS), tensile strength (TS), elongation (EI) and reduction in area (RA) were evaluated after the test (see tab. 2).

Sample	YS [MPa]	TS [MPa]	EI [%]	RA [%]
T22	728.6 ± 2.2	1052.6 ± 3.8	36.7 ± 0.6	33.5 ± 1.8

Table 2. Mechanical properties after tensile test

Fig. 6 shows the engineering stress-strain curves. All samples showed a good combination of high yield strength, ultimate tensile strength and ductility. The high tensile strength is a result of the chromium alloying which, together with a suitably selected recrystallization annealing temperature, helps to produce a fine-grained microstructure and strengthening due to fine precipitated $Cr_{23}C_6$ carbides. The high ductility is a result of the plasticity of the material due to deformation-induced twinning of the austenite grains.

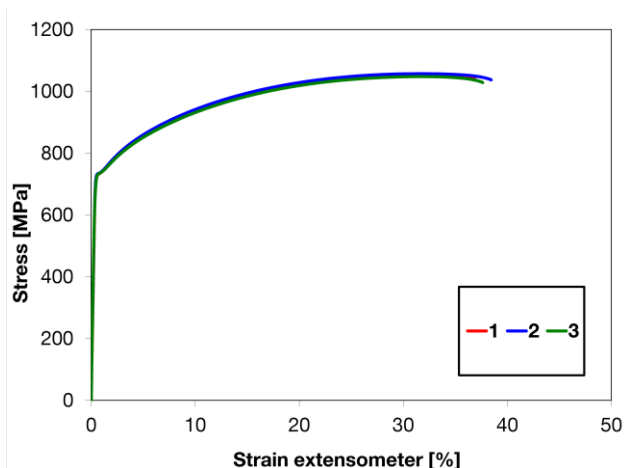


Figure 6. Engineering stress-strain curves of experimental steel

3.3 Corrosion properties

The cyclic polarization curve of annealed experimental steel obtained in model seawater solution containing 3.5 wt. % NaCl at 21 °C is presented in Fig. 7. The corrosion potential (E_{corr}), polarization resistance (R_p) and corrosion current density (i_{corr}) were calculated from the test (Table 3). The values shown in the table are the average values of 3 measurements to obtain statistically relevant results.

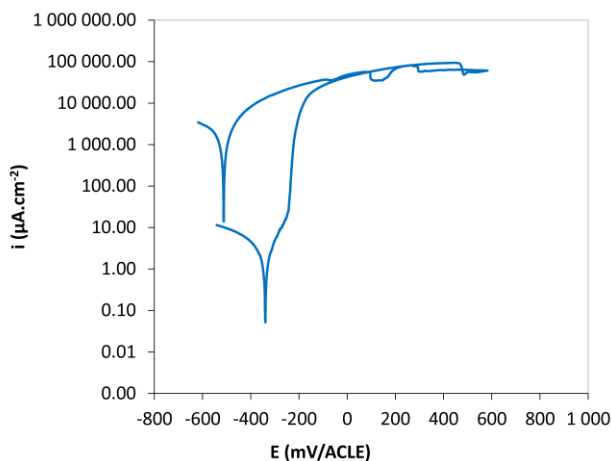


Figure 7. Potentiodynamic polarization curves of annealed experimental steel obtained in model sea water

Sample	E_{corr} [mV/ACLE]	R_p [$\Omega.m^2$]	i_{corr} [$\mu A.cm^{-2}$]
T22	-414.8 ± 5.3	0.19 ± 0.02	0.61 ± 0.11

Table 3. Results of corrosion test

During the test, no substantial surface layer barrier effect was observed. The corrosion resistance of the material studied in this work is higher compared to the corrosion resistance of steels mentioned in the study by Tsay et al. [Tsay 2010], where the steel with 8 % of Cr exhibited the electrochemical parameters E_{corr} of -746 mV and i_{corr} of $3.52 \mu A.cm^{-2}$. Tsay et al.

attributed the decrease in corrosion resistance to the formation of chromium rich carbides. Moreover, the mechanical properties of the present experimental steel with 14.5 Cr are better than above mentioned steel with 8 % of Cr in Tsay et al. study in terms of the ultimate tensile strength (1052.6 MPa here, in comparison to 984 MPa in [Tsay 2010]) and higher ductility (36.7 % here, in comparison to 22.6 % in [Tsay 2010]).

4 CONCLUSION

In this paper the properties of experimental steel with TWIP effect have been investigated. The steel was alloyed with high manganese (29.37 wt.%) and high chromium (14.5 wt.%) content. The experimental melt was cast in a vacuum induction furnace and then hot and cold rolled on an experimental rolling mill. After descaling and subsequent cold rolling, this steel was subjected to recrystallization annealing. Samples taken from the sheets were tested in the laboratory with the focus on microstructural, mechanical and corrosion properties with the following results:

- The crystal phase of the metal matrix of the steel is fully austenitic. No BCC or HPC ferrite (i.e. no alpha or epsilon martensite) were detected, either in the recrystallization annealed condition or in the cold rolled condition. This fact proves that there is no deformation-induced martensite and that the strengthening effect consists of deformation twinning. The small peaks in the XRD patterns indicating the presence of $Cr_{23}C_6$ carbides were found in annealed conditions.
- Recrystallisation annealing at 925 °C for 2 h resulted in a very fine-grained austenitic microstructure with twins. The average grain size measured by EBSD was 15.1 according to ASTM E112.
- This experimental steel achieves a very high tensile strength of 1052.6 ± 3.8 MPa combined with a good elongation of 36.7 ± 0.6 %.
- The i_{corr} parameter reaches the value of $0.61 \pm 0.11 \mu A.cm^{-2}$, which is better value in comparison to the corrosion properties in other studies.

ACKNOWLEDGMENTS

The paper was supported from European Research and Development Fund: Research of advanced steels with unique properties, No. CZ02.1.01/0.0/0.0/16_019/0000836.

This research was also funded by SLOVENIAN RESEARCH AGENCY, grant number P2-0132 and L2-4445.

REFERENCES

- [Cooman 2018] De Cooman, B. C et al. Twinning-induced plasticity (TWIP) steels, Acta Mater. 142, 2018, pp. 283–362. <https://doi.org/10.1016/j.actamat.2017.06.046>
- [Kwon 2010] Kwon, O. et al. New trends in advanced high strength steel developments for automotive application, in: Mater. Sci. Forum, 2010. <https://doi.org/10.4028/www.scientific.net/MSF.638-642.136>.
- [Cornette 2005] Cornette, D. et al. Ultra High Strength FeMn TWIP Steels for automotive safety parts, Rev. Metallurgie, 2005. <https://doi.org/10.1051/metal:2005151>.

[Yuan 2017] Yuan, X. et al. Effect of Cr on mechanical properties and corrosion behaviors of Fe-Mn-C-Al-Cr-N TWIP steels, J. Mater. Sci. Technol, 2017. <https://doi.org/10.1016/j.jmst.2017.08.004>.

[Saad 2007] Saad, A. et al. Manufacturing, mechanical properties and corrosion behaviour of high Mn TWIP steels, Acta Univ. Ouluensis C. 2007.

[Mujica Roncery 2012] Mujica Roncery, L. et al. Mechanical properties of (20-30)Mn12Cr(0.56-0.7)CN corrosion resistant austenitic TWIP steels, in: Steel Res. Int., 2012. <https://doi.org/10.1002/srin.201100316>.

[Mujica 2011] Mujica, L et al. Development and characterization of novel corrosion-resistant TWIP steels, in: Steel Res. Int., 2011. <https://doi.org/10.1002/srin.201000219>.

[Tsay 2010] Tsay, G. et al. A new austenitic FeMnAlCrC alloy with high-strength, high-ductility, and moderate corrosion resistance, Mater. Trans., 2010. <https://doi.org/10.2320/matertrans.M2010199>.

CONTACTS:

Ing. Pavel Podany, Ph.D.

COMTES FHT a.s.

Department of Materials Analysis

Prumyslova 995, Dobruany, 334 41, Czech republic

+420377197340, pavel.podany@comtesfht.cz, www.comtesfht.cz